

# Ophiolitic detritus in Kimmeridgian resedimented limestones and its provenance from an eroded obducted ophiolitic nappe stack south of the Northern Calcareous Alps (Austria)

HANS-JÜRGEN GAWLICK<sup>1</sup>✉, ROMAN AUBRECHT<sup>2</sup>, FELIX SCHLAGINTWEIT<sup>3</sup>,  
SIGRID MISSONI<sup>1</sup> and DUŠAN PLAŠIENKA<sup>4</sup>

<sup>1</sup>Department of Applied Geosciences and Geophysics, Petroleum Geology, Montanuniversität Leoben, Peter Tunner Str. 5, 8700 Leoben, Austria; ✉gawlick@unileoben.ac.at; missoni@unileoben.ac.at

<sup>2</sup>Department of Geology and Paleontology, Faculty of Natural Sciences, Comenius University, Ilkovičova 6, 842 15 Bratislava, Slovak Republic; aubrecht@fns.uniba.sk

Earth Science Institute, Slovak Academy of Sciences, Dúbravská cesta 9, P.O. Box 106, 840 05 Bratislava, Slovak Republic

<sup>3</sup>Lerchenauer Str. 167, 80935 Munich, Germany; EF.Schlagintweit@t-online.de

<sup>4</sup>Department of Geology and Paleontology, Faculty of Natural Sciences, Comenius University, Ilkovičova 6, 842 15 Bratislava, Slovak Republic; plasienska@fns.uniba.sk

(Manuscript received March 14, 2015; accepted in revised form October 25, 2015)

**Abstract:** The causes for the Middle to Late Jurassic tectonic processes in the Northern Calcareous Alps are still controversially discussed. There are several contrasting models for these processes, formerly designated “Jurassic gravitational tectonics”. Whereas in the Dinarides or the Western Carpathians Jurassic ophiolite obduction and a Jurassic mountain building process with nappe thrusting is widely accepted, equivalent processes are still questioned for the Eastern Alps. For the Northern Calcareous Alps, an Early Cretaceous nappe thrusting process is widely favoured instead of a Jurassic one, obviously all other Jurassic features are nearly identical in the Northern Calcareous Alps, the Western Carpathians and the Dinarides. In contrast, the Jurassic basin evolutionary processes, as best documented in the Northern Calcareous Alps, were in recent times adopted to explain the Jurassic tectonic processes in the Carpathians and Dinarides. Whereas in the Western Carpathians Neotethys oceanic material is incorporated in the mélanges and in the Dinarides huge ophiolite nappes are preserved above the Jurassic basin fills and mélanges, Jurassic ophiolites or ophiolitic remains are not clearly documented in the Northern Calcareous Alps. Here we present chrome spinel analyses of ophiolitic detritic material from Kimmeridgian allodapic limestones in the central Northern Calcareous Alps. The Kimmeridgian age is proven by the occurrence of the benthic foraminifera *Protoperoplis striata* and *Labyrinthina mirabilis*, the dasycladalean algae *Salpingoporella pygmaea*, and the alga incertae sedis *Pseudolithocodium carpathicum*. From the geochemical composition the analysed spinels are pleonastes and show a dominance of Al-chromites (Fe<sup>3+</sup>-Cr<sup>3+</sup>-Al<sup>3+</sup> diagram). In the Mg/(Mg + Fe<sup>2+</sup>) vs. Cr/(Cr + Al) diagram they can be classified as type II ophiolites and in the TiO<sub>2</sub> vs. Al<sub>2</sub>O<sub>3</sub> diagram they plot into the SSZ peridotite field. All together this points to a harzburgite provenance of the analysed spinels as known from the Jurassic supra-subduction ophiolites well preserved in the Dinarides/Albanides. These data clearly indicate Late Jurassic erosion of obducted ophiolites before their final sealing by the Late Jurassic-earliest Cretaceous carbonate platform pattern.

**Key words:** heavy minerals, chrome spinel, component analysis, Tethys Ocean, Jurassic Orogen, Eastern Alps.

## Introduction

The aim of this paper is to contribute to the question of the significance of (Middle-to-Late) Jurassic versus solely Early Cretaceous orogenic processes including major thrusting in the Austroalpine unit, and thus also present arguments for the debate on gravitational tectonics (e.g. Mandl 2000, 2013) versus strike-slip tectonics (e.g. Channell et al. 1990, 1992; Frank & Schlager 2006; Ortner et al. 2008) versus obduction related tectonics in the Jurassic of the Austroalpine domain (Gawlick et al. 1999; Faupl & Wagreich 2000; Frisch & Gawlick 2003; Missoni & Gawlick 2011a,b).

For more details concerning the controversial discussion the reader is referred to the publications of Ortner et al. (2008) and Missoni & Gawlick (2011a,b).

In Missoni & Gawlick (2011a,b) invented for the Middle to early Late Jurassic orogenic process along the Neotethys

Ocean the term Neotethyan Belt striking from the Western Carpathians in the north(east) to the Hellenides in the south (compare Schmid et al. 2008; Gawlick et al. 2008), characterized by Middle to early Late Jurassic thrusting triggered by westward or northwestward ophiolite obduction. The thrusting process was sealed by Kimmeridgian to earliest Cretaceous carbonate platforms in the whole realm (Schlagintweit et al. 2008; Gawlick et al. 2012 for the latest reviews).

For the southeasternmost Northern Calcareous Alps and the Western Carpathians Jurassic mélange formation (Meliata mélange and equivalents — Haas et al. 2011 for latest review) is widely accepted. In contrast, for the southern part of the eastern and central Northern Calcareous Alps, this Jurassic mélange formation related to thrusting is still a matter of debate and the Early Cretaceous is still widely seen as the main thrusting event (Schorn et al. 2013). Here the Lower Cretaceous turbiditic Rossfeld Formation with intercalated

mass-flow deposits was interpreted to have been deposited in front of the advancing Juvavic nappes. Recently Krische et al. (2014) also demonstrated that Early Cretaceous thrusting is minor in the southern Calcareous Alps on the basis of the results of component analysis of the Early Cretaceous mass flows in the Rossfeld Formation (compare Gawlick et al. 2008; Missoni & Gawlick 2011a,b).

One argument for an Early Cretaceous thrusting is the occurrence of detrital chrome spinel grains (Faupl & Pober 1991) in the sedimentary rocks of the Early Cretaceous foreland basin fills (Rossfeld Basins) and their absence in older strata beside a lot of geochronological age data in the crystalline basement (Frank 1987), and from several areas of the southern Northern Calcareous Alps with thermal overprint (Kralik et al. 1997; Frank & Schlager 2006). In addition, late Early Cretaceous to early Late Cretaceous thrusting processes including ultra-high-pressure conditions (Janák et al. 2004; Thöni 2006) in the crystalline basement are well known. Janák et al. (2004) presented lithosphere kinematic reconstructions of the Austroalpine system. However, these late Early Cretaceous to early Late Cretaceous tectonics are slightly younger than the youngest sediments in the Rossfeld Basin (Early–Middle Aptian — Fuchs 1968; Weidich 1990; Schlagintweit et al. 2012). Moreover, deposition of the Rossfeld Formation stopped contemporaneously with the onset of the late Early Cretaceous to early Late Cretaceous tectonic event, showing clearly that the Jurassic orogeny and the late Early Cretaceous to early Late Cretaceous orogeny must be clearly separated.

Missoni & Gawlick (2011a) pointed out the existence of detrital chrome spinel grains in the Late Kimmeridgian but without geochemical analyses. The reason for the still missing detailed analysis was the lack of their occurrence in investigateable quantities. To fill the gap, we present analyses of ophiolitic detritic material from Kimmeridgian silicified allodapic limestones from the Saalach Zone in the central Northern Calcareous Alps (Fig. 1).

## Geological setting

The study area is located southwest of Salzburg, south of the township Unken (Fig. 1) and north-northwest of Mount Dietrichshorn (Fig. 2) and belongs to the Hallstatt Mélange area of the Saalach zone (Tollmann 1985) or Saalach Fault Zone (Frisch & Gawlick 2003). A more detailed geological sketch map of the area was recently published by Ortner et al. (2008) and for details the reader is referred to Fig. 2 in Ortner et al. (2008). In Fig. 2 the former interpretation (Ortner et al. 2008) of the investigated rocks as Early Cretaceous (Valanginian–Barremian) is indicated. In contrast, our reinvestigation of some of these rocks gives evidence for the Kimmeridgian age. This means, that the strike-slip fault separating the Saalach Zone Unit from the Tirolic Unit to the west is slightly west of the studied localities, cutting here through similar lithologies, the Rossfeld (=Lackbach) Formation to the west and the Sillenkopf Formation to the east. By following this strike-slip fault, for example, to the north, the separation of the

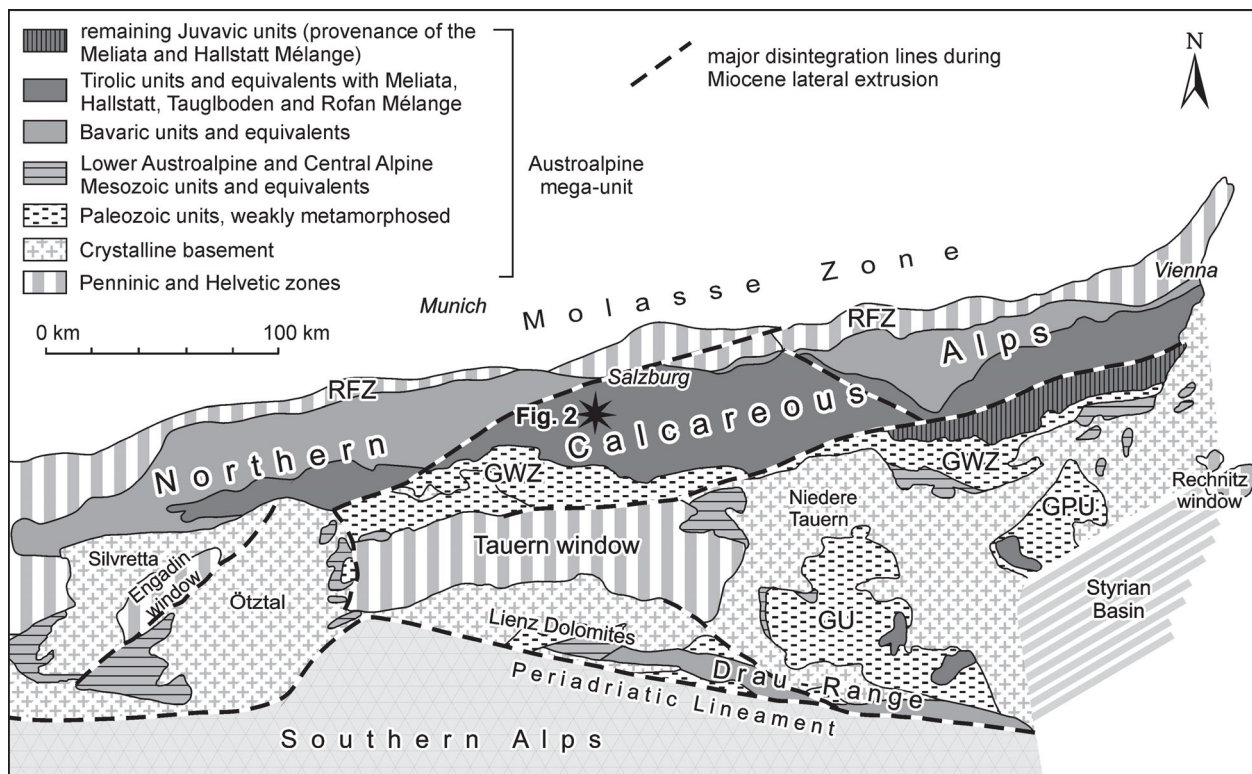
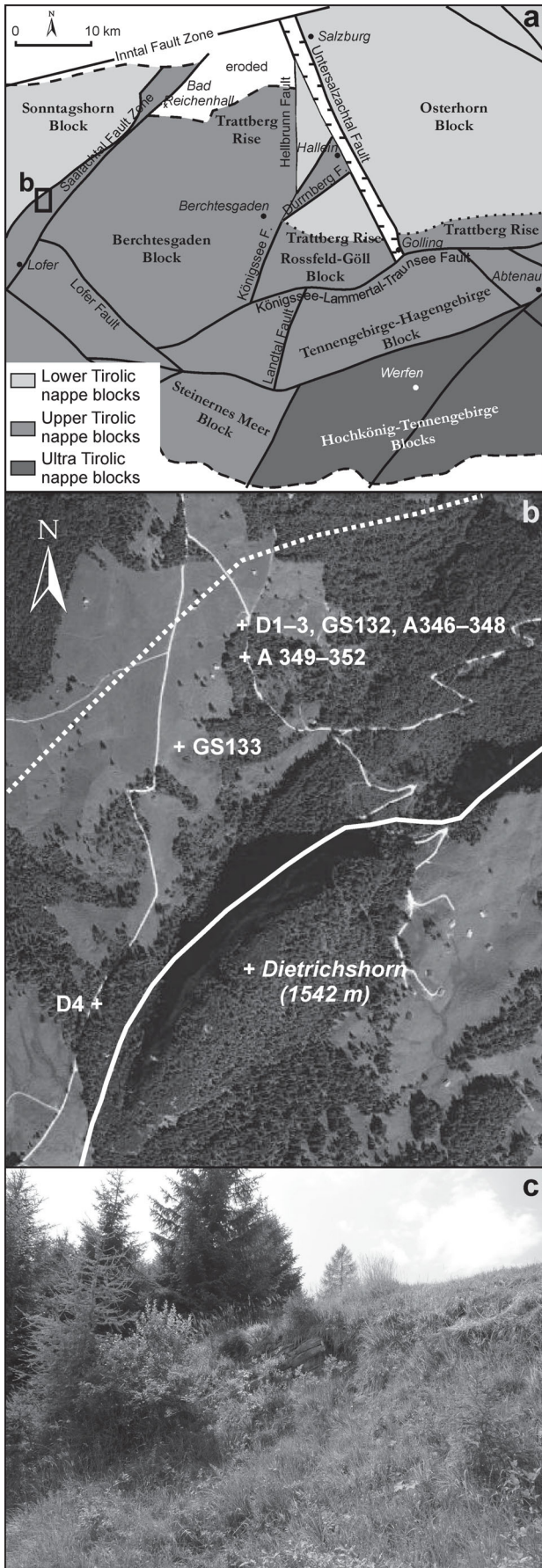


**Fig. 1.** Tectonic sketch map of the Eastern Alps and study area (black star) southwest of Salzburg (after Tollmann 1977; Frisch & Gawlick 2003). GPU — Graz Paleozoic Unit, GU — Gurktal Unit, GWZ — Greywacke Zone, RFZ — Rhenodanubian Flysch Zone.



two units became much clearer: here the Hallstatt Mélange occurs directly beside the Rossfeld (=Lackbach) Formation.

Mount Dietrichshorn consists of Kimmeridgian-Tithonian shallow-water carbonates (Darga & Schlagintweit 1991) of the southern Plassen Carbonate Platform (Lärchberg Carbonate Platform — Gawlick et al. 2009), later overthrust — most probably in the latest Tithonian — above the studied Kimmeridgian resediments (=line in Fig. 2b, formerly interpreted as the boundary between the Saalach Unit and the Tirolic Unit — Ortner et al. 2008). The investigated resediments are attributed to the Sillenkopf Formation (Fig. 3), which was deposited in a deep-water basin between the Lärchberg Carbonate Platform to the south and the Plassen Carbonate Platform s. str. to the north (Fig. 3). Therefore the boundary between the Saalach Unit and the Tirolic Unit must be situated more to the northwest (dotted line). The exact position cannot be mapped in the grassland area without dense sampling. For more stratigraphic and sedimentological details the reader is recommended to consult papers by Gawlick et al. (2009), Pestal et al. (2009) and the references therein. For the reconstruction of the Jurassic to Early Cretaceous geodynamic history the reader is recommended to look at papers by Missoni & Gawlick (2011a,b) and Gawlick et al. (2012).

**Sampled sites, material and methods**

Beside several smaller outcrops along the forest road and in the grassland area, the main sampled outcrop is located on a forest road north of Mount Dietrichshorn (Fig. 2). About 2 m of relatively thin-bedded series of allodapic limestones are exposed here as a result of artificial digging (Fig. 3). For heavy mineral investigations three samples were taken from various beds (samples D1-3). For stratigraphic and microfacies investigations the more coarse-grained carbonatic resediments were taken. Additional samples of the same formation were taken in the wider surroundings northwest and west of Mount Dietrichshorn (Fig. 2).

For heavy mineral investigations, the samples were crushed, washed and sieved to get the sandy fraction (0.08-1 mm).

**Fig. 2.** a — recent block configuration of the western part of the central northern Calcareous Alps with major faults active during Miocene lateral tectonic extrusion after Frisch & Gawlick (2003) and study area; b — position of the sampling sites. Topographic background photo from Google Earth (2014). The white line should mark the boundary between the Late Jurassic shallow-water platform carbonates of Mount Dietrichshorn and the Early Cretaceous sedimentary rocks to the west and is interpreted as a normal fault according to Ortner et al. (2008). In fact the dotted line is the thrust plane of Mount Dietrichshorn above the Sillenkopf Formation. All Kimmeridgian samples plot into this area. The strike-slip fault separating the Sillenkopf Formation from the Lackbach Formation must be located in the northeastern grassland area (dotted line). See text for explanation; c — outcrop situation in the year 2012. The artificial digging from the year 2006 (first sampling campaign) is mostly covered. Along the forest road several similar outcrops exist, with the same dipping below Mt Dietrichshorn (eastward). In contrast, the Lackbach Formation shows a westward dipping.

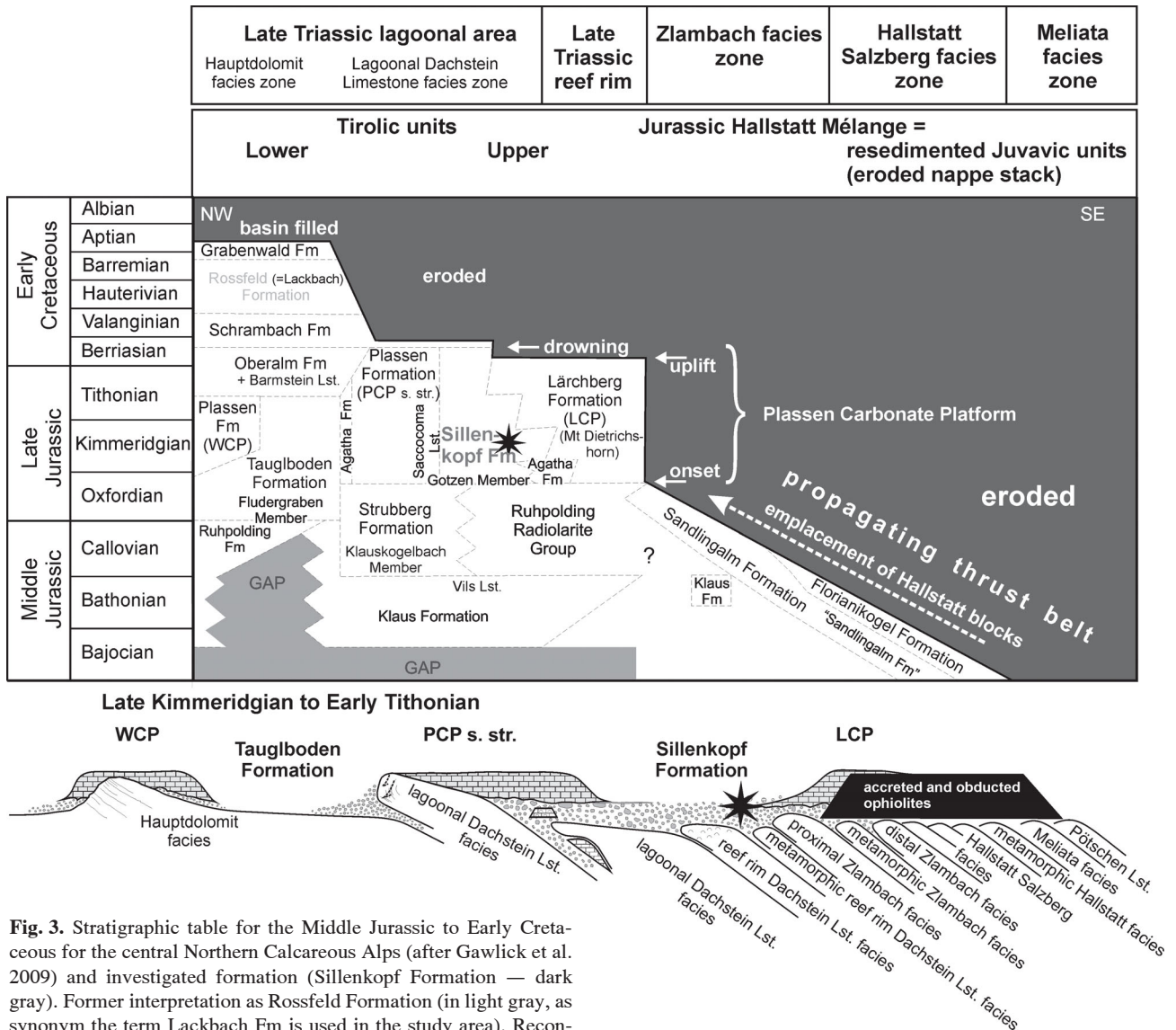


**Fig. 3.** Stratigraphic table for the Middle Jurassic to Early Cretaceous for the central Northern Calcareous Alps (after Gawlick et al. 2009) and investigated formation (Sillenkopf Formation — dark gray). Former interpretation as Rossfeld Formation (in light gray, as synonym the term Lackbach Fm is used in the study area). Reconstruction of the Kimmeridgian paleotopographic situation (after Missoni & Gawlick 2011b; Gawlick et al. 2012): After the late Middle to early Late Jurassic compressional tectonics a nappe stack was formed. From latest Oxfordian times onwards several carbonate platforms started to evolve, the Wolfgangsee Carbonate Platform in the north, the Plassen Carbonate Platform in a central position, and the Lärchberg Carbonate Platform in the south. Between the platforms deep-water basins remain, e.g. between the Plassen Carbonate Platform s. str. and the Lärchberg Carbonate Platform the Sillenkopf Basin (Sillenkopf Fm). The Sillenkopf Basin receives material from the obducted ophiolite nappe stack and the shallow-water carbonate platform on top.

The heavy minerals were separated in bromoform (density ca. 2.8). The 0.08–0.25 mm fraction was studied by transmitted light; the whole fraction was also examined under a binocular microscope. Percentage ratios of the heavy mineral assemblages were determined by ribbon point counting. Subsequently, the spinel grains were hand-picked, mounted using epoxide resin and polished for microprobe analysis.

The chemical compositions of the spinels and the inclusions inside them were determined using a CAMECA SX-100 electron microprobe at the State Geological Institute of Dionýz Štúr in Bratislava. The analytical conditions were as follows: 15 kV accelerating voltage, 20 nA beam current and a beam diameter of 5 µm. Raw counts were corrected using an X-PHI routine. Standards: Al — Al<sub>2</sub>O<sub>3</sub>, Mg — forsterite,

Si — wollastonite, Ti — TiO<sub>2</sub>, Ca — wollastonite, Fe — fayalite, Mn — rodonite, Cr — Cr, Ni — Ni, V — V, Zn — willemite. For all standards, the K $\alpha$  spectral line was used.

**Lithology, stratigraphy and microfacies**

The studied succession west of Mount Dietrichshorn consists of carbonatic sandstones in parts with graded bedding, intercalated coarser grained resedimented limestones and wacke- to packstones, rich in spicula or radiolarians. In parts the beds are completely silicified.

The age determination was done on the basis of shallow-water organisms from the intercalated limestone resediments

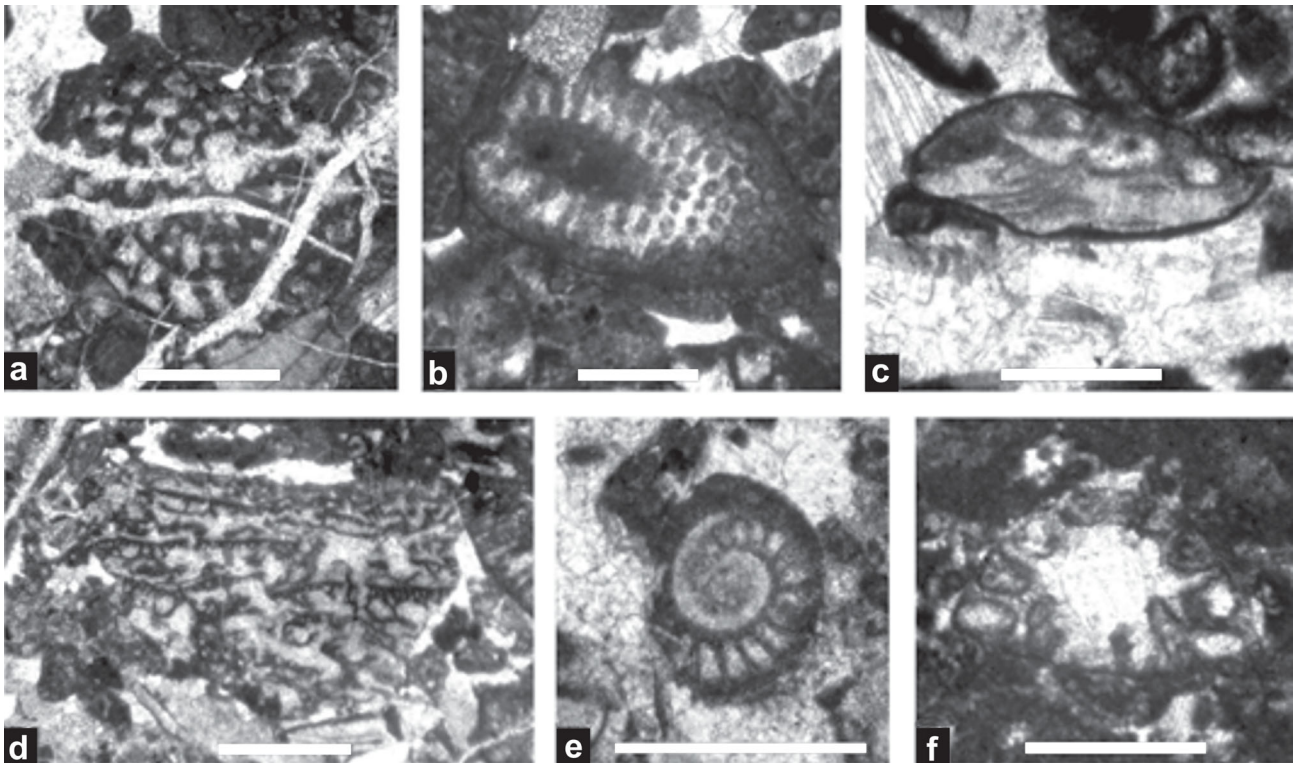


**Fig. 4.** Microfossils of the Kimmeridgian allodapic limestones (sample GS132). **a** — benthic foraminifer *Labyrinthina mirabilis* Weynschenk, **b** — Dasycladale *Salpingoporella pygmaea* (Gümbel), **c** — benthic foraminifer *Mohlerina basiliensis* (Mohler), **d** — incertae sedis *Pseudolithocodium carpathicum* Misik, **e** — benthic foraminifer *Protopenneroplis striata* Weynschenk, **f** — benthic foraminifer *Coscinoconus* cf. *alpinus* Leupold. Scale bars = 0.5 mm.

(Figs. 4, 5). Determinable organisms occur only in the coarser-grained allodapic limestones with only few chrome spinels, whereas in the finer-grained resediments the organisms are highly fragmented but the chrome spinels are relatively enriched. Notably the association of the benthic foraminifera *Protopenneroplis striata* Weynschenk (Fig. 4e) and *Labyrinthina mirabilis* Weynschenk (Fig. 4f) are typically associated with high-energy platform margin depositional settings, such as shoals, from where they became resedimented downslope into basinal sequences. The resedimented dasycladale *Salpingoporella pygmaea* (Gümbel) (Fig. 4b) and the alga incertae sedis *Pseudolithocodium carpathicum* Misik (Fig. 4d) are typically associated with near-reefal to reefal facies of external platform facies. A Kimmeridgian age can be deduced from the occurrence of *L. mirabilis* and the general Alpine shallow-water facies evolution (Schlagintweit et al. 2005, for details).

Debris of younger, Late Tithonian/?Early Berriasian shallow-water bioclasts is found in the Lackbach Formation with the occurrence of the larger benthic foraminifer *Anchispirocyclina lusitanica* (Egger) (Darga & Weidich 1986). Allochthonous older clasts beside the Late Jurassic shallow-water clasts are missing. The resediments consist exclusively of shallow-water to slope material as is typical for the early onset of the Lärchberg Carbonate Platform. These resediments are similar to the resediments of the type area of the Sillenkopf Formation (Missoni et al. 2001; Gawlick & Frisch 2003), but without Triassic clasts. Similar resediments are also known from the early Kurbnesh Platform in Albania

(Schlagintweit et al. 2008), where Kimmeridgian resediments of the early platform stage contain ophiolite debris. The studied succession resembles a proximal counterpart of the Sillenkopf Formation of the type-locality in Berchtesgaden (Missoni et al. 2001; Gawlick et al. 2009), but deposited much nearer to the Lärchberg Carbonate platform (Fig. 3).

The overall lithology and macroscopic lithofacies are therefore quite similar to the Lower Cretaceous Rossfeld Formation (here = Lackbach Formation of Darga & Weidich 1986). The main lithological difference is the occurrence of relatively coarse-grained resedimented limestones missing in the Early Cretaceous successions. In the Lackbach Formation only fine- to coarse-grained breccia layers with older clasts, also of Late Jurassic age, occur (Darga & Weidich 1986). In contrast to the overall lithology, the microfacies characteristics of this series differ significantly (component and organism spectrum) from the Rossfeld (=Lackbach) Formation to the west, in detail described and dated by Darga & Weidich (1986). The underlying succession does not directly outcrop in the study area, but further to the north- or southeast the Kimmeridgian strata are underlain by the Hallstatt Mélange (Missoni & Gawlick 2010; Quast et al. 2010).

#### *Description of the investigated samples for heavy mineral analysis*

The microscopic analysis shows that the sediment is represented by silicified, finely laminated allodapic limestone. The

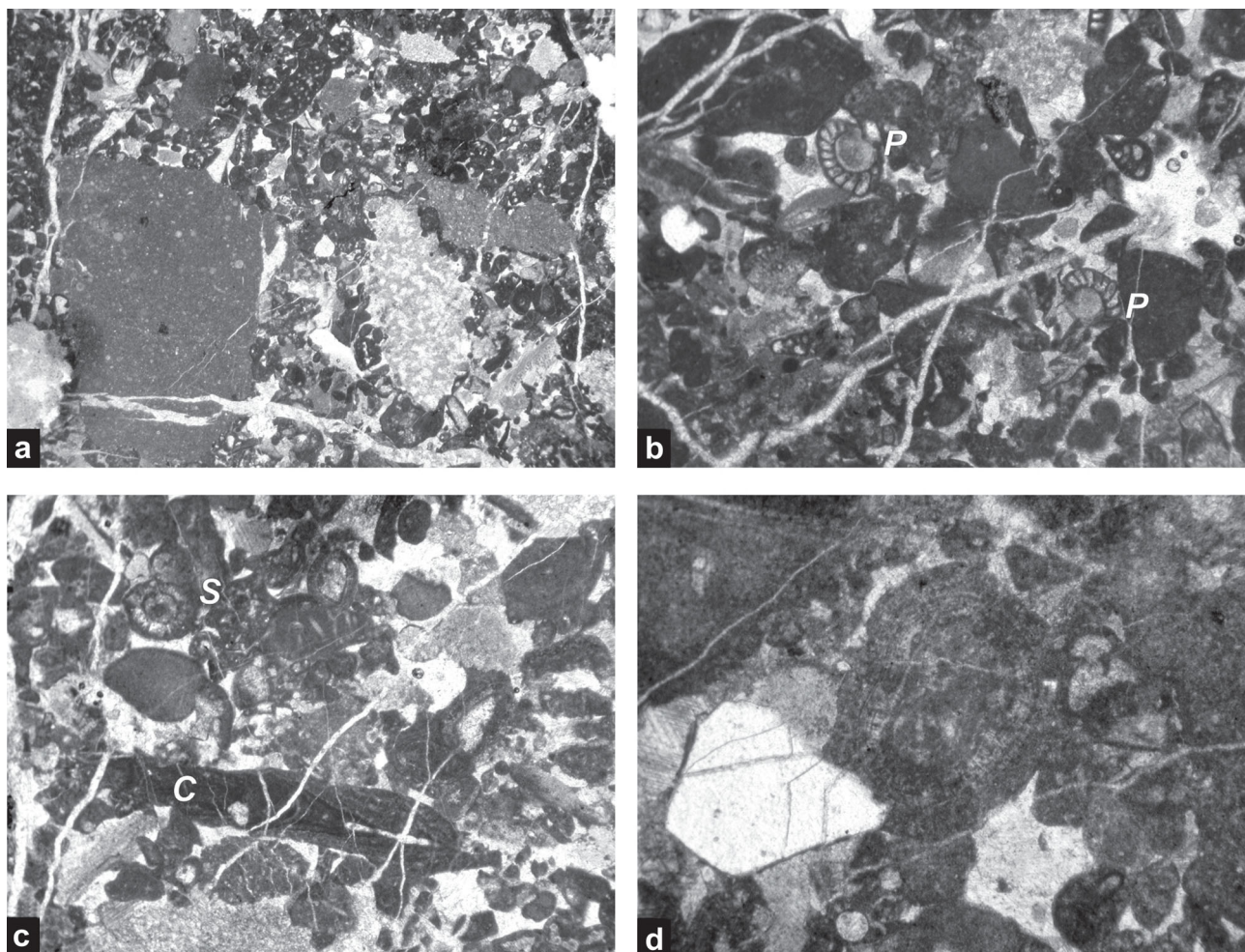


**Fig. 5.** Microfacies of the studied allodapic limestones (samples GS132, A346–352). **a** — poorly sorted packstone with benthic foraminifera, debris of corals and a large radiolarian wackestone lithoclast, which resembles the basal microfacies of the Sillenkopf Formation. Width of photo: 1.4 cm; **b** — magnified view of a grain-/packstone with two specimens of *Protopeneroplis striata* Weynschenk. Width of photo: 0.5 cm; **c** — grain-/packstone with incertae sedis *Crescentiella morronensis* (Crescenti) (C) and dasycladale *Salpingoporella pygmaea* (Gümbel) (S); Width of photo: 1.4 cm; **d** — magnified view with ooids and a subangular quartz grain. Width of photo: 0.25 cm.

sediment is well-sorted, with mean size of allochems ranging between 50–100  $\mu\text{m}$  (Fig. 6a). The majority of the allochems are represented by silicisponge spicula (rhaxa, monaxone to bizarre skeletons of lithistid sponges) and radiolarians (Fig. 6b). Agglutinated textulariid foraminifers (Fig. 6c–e) and some planispiral foraminifers are quite common (Fig. 6f). The samples also contain rare tiny echinoderm particles and indeterminate, yellowish, probably phosphatic particles. Some allochems bear signs of very fine, probably bacterial borings filled with opaque diagenetic Fe–Mn minerals. Siliciclastic admixture is represented by uncommon dispersed fine-grained quartz sand grains, in places accompanied by tiny muscovite scales. From heavy minerals, spinel grains (Fig. 6g) and rare zircons are visible in thin-sections (details of the heavy mineral analysis below). The deposit contains pyrite seams to swarms, filling small pores along the lamination. Diagenetic overprint of the sediment is quite strong. It is pervasively silicified, with silicification being rather selective than frontal. The entire rock is penetrated by thin blocky-cal-

cite veinlets, also cutting through the silicified parts. This indicates that the veinlets are the latest diagenetic phenomenon.

## Heavy minerals

### Percentage ratios of heavy minerals

The heavy mineral fraction is strongly dominated by spinels, the percentage of which varies between 93 and 98 % (Table 1). Other minerals occur subordinately; they are represented mostly by garnet, varying in the range of 0–4 %. Other heavy minerals — zircon, rutile and tourmaline vary from 0 to maximum 2 %.

### Chemical composition of detrital spinels and their origin

The spinel grains were mostly fragmented; their roundness is low (the grains are mostly subangular). The majority show

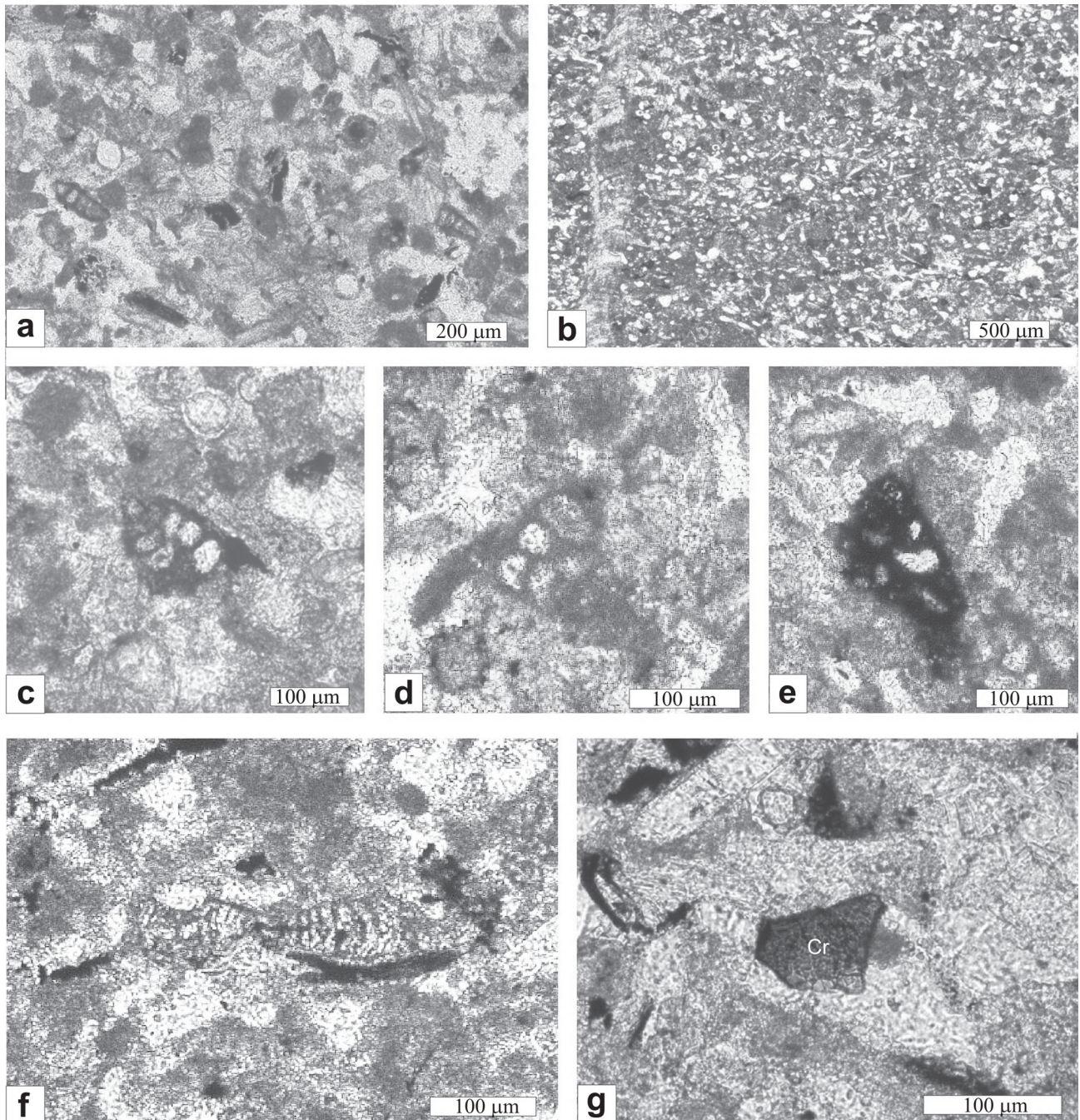


**Fig. 6.** Microfacies of the sampled silicified allodapic limestones. **a** — well-sorted organodetrital sediment forming the main portion of the examined allodapic limestones, **b** — parts of the rocks representing the fine-grained matrix consist of spiculitic-radiolarian microfacies, **c-e** — Textulariids are the most common foraminifers in the sediment, **f** — *Spirillina* sp., **Cr** — detritic chrome spinel grain.

no zonation. Only some grains had alteration rims (Fig. 7a-c). Some spinel grains have inclusions of other minerals, such as ortho- and clinopyroxenes and various types of chlorites and amphiboles (Fig. 7d-f).

The analysed spinels show some chemical variability, mainly in the most important elements which are diagnostic of their provenance, such as Mg, Fe, Cr, Al, and Ti (Table 2). Two types of diagrams are widely used for this purpose: (1)  $Mg/(Mg+Fe^{2+})$  vs.  $Cr/(Cr+Al)$ , and (2)  $Al_2O_3$  vs.  $TiO_2$ .

The first one was introduced by Dick & Bullen (1984), who distinguished three fields in their diagram: 1) Type I ophiolites which correspond to peridotite for which  $Cr/(Cr+Al)$  in spinel does not exceed 0.60. These peridotites evolved in mid-oceanic ridge settings; 2) Type III ophiolites representing peridotites bearing spinel with  $Cr/(Cr+Al)$  above 0.60, which are related to the early stages of arc formation on oceanic crust; 3) Type II ophiolites bearing spinels with a wide range of  $Cr/(Cr+Al)$ , representing transitional phases. Based

Table 1: Percentage ratio of heavy minerals in the examined samples.

| Analysis no.                   | Fresh spinels      |       |       |       |       |       |       |       |       |       |       |      |       |       |       | Volcanic spinels |       |       | Altered spinels |       |  |
|--------------------------------|--------------------|-------|-------|-------|-------|-------|-------|-------|-------|-------|-------|------|-------|-------|-------|------------------|-------|-------|-----------------|-------|--|
|                                | Peridotite spinels |       |       |       |       |       |       |       |       |       |       |      |       |       |       | X                | 27/1  | X1    | X2              | Y1    |  |
|                                | 1/1                | 5/1   | 8/1   | 11/1  | 12/1  | 13/1  | 14/1  | 15/1  | 16/1  | 19/1  | 20/1  | Y    |       |       |       |                  |       |       |                 |       |  |
| SiO <sub>2</sub>               | 0.03               | 0.03  | 0.15  | 0.00  | 0.00  | 0.05  | 0.02  | 0.00  | 0.02  | 0.01  | 0.01  | 0.03 | 0.00  | 0.00  | 0.00  | 0.00             | 0.00  | 0.02  | 0.03            | 0.07  |  |
| TiO <sub>2</sub>               | 0.08               | 0.12  | 0.07  | 0.06  | 0.07  | 0.07  | 0.05  | 0.10  | 0.11  | 0.07  | 0.03  | 0.05 | 0.35  | 0.44  | 0.35  | 0.44             | 0.76  | 0.03  | 0.03            | 0.12  |  |
| Al <sub>2</sub> O <sub>3</sub> | 26.43              | 21.50 | 20.35 | 22.75 | 23.20 | 20.41 | 33.58 | 25.49 | 18.91 | 19.43 | 26.83 | 20   | 26.89 | 18.58 | 26.89 | 18.58            | 10.49 | 0.15  | 0.15            | 0.85  |  |
| Cr <sub>2</sub> O <sub>3</sub> | 43.26              | 46.79 | 48.59 | 45.65 | 45.30 | 49.92 | 35.91 | 44.87 | 51.39 | 48.59 | 42.99 | 49.3 | 41.12 | 44.30 | 41.12 | 44.30            | 46.65 | 4.33  | 4.33            | 46.25 |  |
| FeO                            | 14.40              | 18.79 | 17.37 | 18.02 | 18.29 | 16.66 | 15.58 | 17.11 | 17.57 | 19.00 | 15.30 | 17.7 | 17.38 | 25.84 | 17.38 | 25.84            | 34.31 | 88.23 | 45.32           | 45.32 |  |
| MnO                            | 0.32               | 0.34  | 0.32  | 0.35  | 0.33  | 0.39  | 0.34  | 0.29  | 0.37  | 0.36  | 0.34  | 0.34 | 0.28  | 0.43  | 0.28  | 0.43             | 0.72  | 0.04  | 0.04            | 1.06  |  |
| MgO                            | 14.87              | 11.92 | 12.58 | 12.14 | 12.33 | 12.54 | 14.51 | 13.09 | 12.51 | 11.95 | 13.66 | 11.9 | 13.47 | 9.45  | 13.47 | 9.45             | 4.90  | 0.00  | 0.00            | 2.07  |  |
| V <sub>2</sub> O <sub>5</sub>  | 0.25               | 0.19  | 0.26  | 0.26  | 0.26  | 0.20  | 0.22  | 0.19  | 0.18  | 0.23  | 0.20  | 0.22 | 0.20  | 0.35  | 0.20  | 0.35             | 0.25  | 0.00  | 0.00            | 0.21  |  |
| NiO                            | 0.11               | 0.06  | 0.05  | 0.09  | 0.13  | 0.03  | 0.14  | 0.09  | 0.08  | 0.09  | 0.09  | 0.01 | 0.13  | 0.10  | 0.13  | 0.10             | 0.07  | 0.00  | 0.00            | 0.10  |  |
| ZnO                            | 0.06               | 0.11  | 0.14  | 0.13  | 0.19  | 0.13  | 0.19  | 0.15  | 0.08  | 0.14  | 0.20  | 0.12 | 0.16  | 0.12  | 0.16  | 0.12             | 0.24  | 0.06  | 0.06            | 0.24  |  |
| sum                            | 99.8               | 99.9  | 99.9  | 99.4  | 100.1 | 100.4 | 100.5 | 101.4 | 101.2 | 99.9  | 99.6  | 99.5 | 100.0 | 99.6  | 100.0 | 99.6             | 98.4  | 92.9  | 96.3            | 96.3  |  |
| Si                             | 0.00               | 0.00  | 0.00  | 0.00  | 0.00  | 0.00  | 0.00  | 0.00  | 0.00  | 0.00  | 0.00  | 0.00 | 0.00  | 0.00  | 0.00  | 0.00             | 0.00  | 0.00  | 0.00            | 0.00  |  |
| Ti                             | 0.00               | 0.00  | 0.00  | 0.00  | 0.00  | 0.00  | 0.00  | 0.00  | 0.00  | 0.00  | 0.00  | 0.00 | 0.00  | 0.00  | 0.00  | 0.00             | 0.00  | 0.00  | 0.00            | 0.00  |  |
| Al                             | 0.93               | 0.79  | 0.75  | 0.83  | 0.84  | 0.75  | 1.15  | 0.90  | 0.69  | 0.72  | 0.95  | 0.74 | 0.95  | 0.70  | 0.95  | 0.70             | 0.43  | 0.01  | 0.04            | 0.04  |  |
| Cr                             | 1.02               | 1.15  | 1.19  | 1.12  | 1.10  | 1.22  | 0.82  | 1.06  | 1.26  | 1.20  | 1.02  | 1.22 | 0.98  | 1.12  | 0.98  | 1.12             | 1.27  | 1.13  | 1.37            | 1.37  |  |
| Fe <sup>2+</sup>               | 0.32               | 0.43  | 0.40  | 0.42  | 0.42  | 0.41  | 0.36  | 0.40  | 0.41  | 0.43  | 0.37  | 0.43 | 0.38  | 0.53  | 0.38  | 0.53             | 0.72  | 1.00  | 0.84            | 0.84  |  |
| Fe <sup>3+</sup>               | 0.04               | 0.05  | 0.05  | 0.04  | 0.05  | 0.02  | 0.02  | 0.03  | 0.05  | 0.07  | 0.02  | 0.03 | 0.06  | 0.16  | 0.06  | 0.16             | 0.27  | 1.86  | 0.58            | 0.58  |  |
| Mn                             | 0.01               | 0.01  | 0.01  | 0.01  | 0.01  | 0.01  | 0.01  | 0.01  | 0.01  | 0.01  | 0.01  | 0.00 | 0.01  | 0.01  | 0.01  | 0.01             | 0.02  | 0.00  | 0.03            | 0.03  |  |
| Mg                             | 0.66               | 0.55  | 0.58  | 0.56  | 0.56  | 0.58  | 0.63  | 0.59  | 0.58  | 0.56  | 0.61  | 0.56 | 0.60  | 0.45  | 0.60  | 0.45             | 0.25  | 0.00  | 0.12            | 0.12  |  |
| V                              | 0.01               | 0.00  | 0.01  | 0.01  | 0.01  | 0.01  | 0.01  | 0.01  | 0.00  | 0.00  | 0.00  | 0.01 | 0.00  | 0.01  | 0.00  | 0.01             | 0.01  | 0.00  | 0.01            | 0.01  |  |
| Ni                             | 0.00               | 0.00  | 0.00  | 0.00  | 0.00  | 0.00  | 0.00  | 0.00  | 0.00  | 0.00  | 0.00  | 0.00 | 0.00  | 0.00  | 0.00  | 0.00             | 0.00  | 0.00  | 0.00            | 0.00  |  |
| Zn                             | 0.00               | 0.00  | 0.00  | 0.00  | 0.00  | 0.00  | 0.00  | 0.00  | 0.00  | 0.00  | 0.00  | 0.00 | 0.00  | 0.00  | 0.00  | 0.00             | 0.00  | 0.00  | 0.00            | 0.00  |  |
| sum                            | 3.00               | 3.00  | 3.00  | 3.00  | 3.00  | 3.00  | 3.00  | 3.00  | 3.00  | 3.00  | 3.00  | 3.00 | 3.00  | 3.00  | 3.00  | 3.00             | 3.00  | 3.00  | 3.00            | 3.00  |  |
| Mg/(Mg+Fe <sup>2+</sup> )      | 0.67               | 0.56  | 0.59  | 0.57  | 0.57  | 0.59  | 0.64  | 0.59  | 0.64  | 0.59  | 0.62  | 0.56 | 0.61  | 0.46  | 0.61  | 0.46             | 0.26  | 0.00  | 0.12            | 0.12  |  |
| Cr/(Cr+Al)                     | 0.52               | 0.59  | 0.62  | 0.57  | 0.57  | 0.62  | 0.42  | 0.54  | 0.65  | 0.63  | 0.52  | 0.62 | 0.51  | 0.62  | 0.51  | 0.62             | 0.75  | 0.95  | 0.95            | 0.97  |  |

Table 2: Representative microprobe analyses of the spinels (in wt. %). Formula is based on 3 cations.

| Sample | Spinel | Garnet | Zircon | Rutile | Tourmaline |
|--------|--------|--------|--------|--------|------------|
| D1     | 93     | 4      | 1      | 2      | 1          |
| D2     | 98     | 1      | 0      | 0      | 0          |
| D3     | 97     | 2      | 1      | 0      | 0          |
| D4     | 97     | 0      | 1      | 0      | 0          |

on these classifications, Pober & Faupl (1988) discriminated spinels derived from harzburgite and lherzolite rocks.

To distinguish the spinels derived from peridotites and volcanics, a diagram of TiO<sub>2</sub> vs. Al<sub>2</sub>O<sub>3</sub> is used (Lenaz et al. 2000; Kamenetsky et al. 2001). More than 95 % of spinel from mantle rocks has TiO<sub>2</sub> lower than 0.2 wt. %, and volcanic spinel with TiO<sub>2</sub> lower than 0.2 wt. % is uncommon, the boundary between peridotitic and volcanic spinels was set at a TiO<sub>2</sub> value of 0.2 wt. % (for overview see Lenaz et al. 2009).

On the basis of the chromite-magnesio spinel prism (Fig. 8a) for the solid solution spinel-hercynite-chromite-magnesiochromitemagnesioferri-rite-magnetite, two chemical variation diagrams were constructed by Gargiulo et al. (2013) with the projections on the triangular face "b" of the spinel prism (Fig. 8b) and the compositions on the left-lateral face "c" of the prism (Fig. 8c). The diagrams were constructed on the base of previously published diagrams of Stevens (1944), Haggerty (1991) and Deer et al. (1992). In the triangular, Fe<sup>3+</sup>-Cr-Al diagram (Fig. 8b), the analysed spinels plot mostly in the Al-chromite field and less in the picotite field. A single primary grain plot also in the chromite field. In the binary diagram (Fig. 8c), all the primary grains plot exclusively in the pleonaste field.

Only some altered zones show shifting towards Cr and Fe, forming ferrian-chromite (ferrian pleonaste) to magnetite. Such pattern is typical for ophiolite alteration, such as serpentinization (see Mikuš & Spišák 2007).

In the Mg/(Mg+Fe<sup>2+</sup>) vs. Cr/(Cr+Al) diagram, distribution of the fresh spinels best match the field of type II ophiolites (Fig. 9a) of Dick & Bullen (1984); in the same diagram of Pober & Faupl (1988), they best match the field of harzburgites (Fig. 9b).

In the TiO<sub>2</sub> vs. Al<sub>2</sub>O<sub>3</sub> of Lenaz et al. (2000) and Kamenetsky et al. (2001), most of the fresh spinel grains fall into peridotite fields (with TiO<sub>2</sub> of less than 0.2 wt. %); only two measured values had higher TiO<sub>2</sub> values, falling into the fields of back-arc basin and mid-oceanic ridge volcanics (Fig. 10). The altered zones in spinels are shifted towards low-Al values in this diagram. The peridotitic spinels show mostly lower Al<sub>2</sub>O<sub>3</sub> values, which match the supra-subduction zone peridotites field.

## Discussion

The chemistry of spinels revealed their provenance from harzburgitic sources, which means from the oceanic crust that originated rather in arc to back-arc or suprasubduction ophiolites (SSZ) setting rather than in mid-oceanic ridge. Harzburgitic sources vastly predominate in most of the Cre-

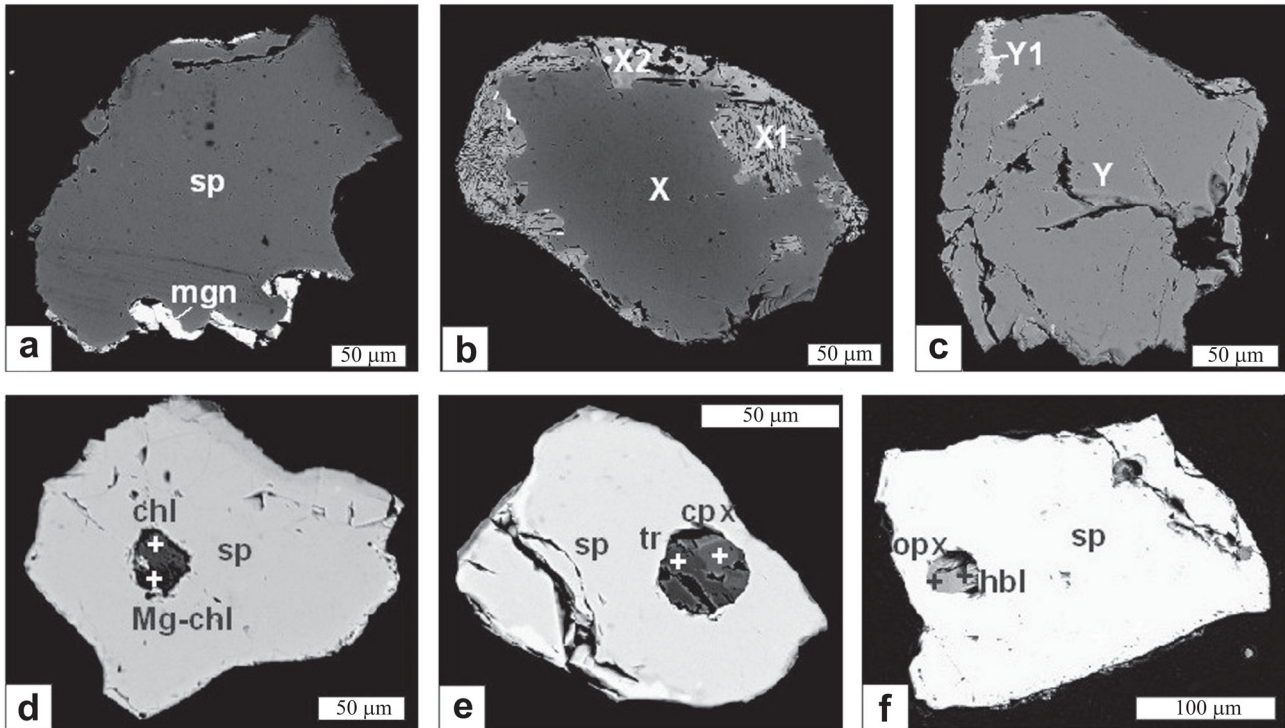


**Fig. 7. a–c** — photographs of spinel grains with altered rims. Abbreviations: sp — spinel, mgn — magnetite, X, X1, X2, Y, Y1 — measurement points corresponding to the measurements plotted in the diagrams of Fig. 4 and Fig. 6; **d–f** — examples of inclusions in spinel grains. Explanations: chl — chlorite, Mg-chl — clinocllore, tr — tremolite, cpx — clinopyroxene, opx — orthopyroxene, hbl — homblende.

taceous synorogenic flyschs all over the Alpine-Carpathian-Dinaridic belt (Poher & Faupl 1988; Árgyelán 1996; von Eynatten & Gaupp 1999; Jablonský et al. 2001; Lužar-Oberiter et al. 2009).

There are some cases described in literature which showed that the  $Mg/(Mg+Fe^{2+})$  vs.  $Cr/(Cr+Al)$  provenance diagrams of Dick & Bullen (1984) and Poher & Faupl (1988) are not necessarily valid for all spinel sources. Power et al. (2000) introduced a case from the Rum layered intrusion in the Inner Hebrides, Scotland, where they revealed a wide spectrum of spinels from chromite seams, covering the entire  $Mg/(Mg+Fe^{2+})$  vs.  $Cr/(Cr+Al)$  diagram. They also recorded a strong shift of spinel chemistry towards Cr- and Fe-enrichment, versus Al-depletion in the grains separated from sediments of the streams draining the intrusion body. The latter they explained by a strong influx of spinels coming from the wall-rock where they were dispersed and not sampled primarily. However, Barnes & Roedes (2001) showed, that the environment of layered intrusions is special in displaying an unusual Al-increasing and Fe-decreasing trend with falling temperature which is opposite to normal. This is also responsible for scattering of the values in diagrams bigger than in ophiolitic sources. We may therefore substantially suppose, that there is still a provenance value of the  $Mg/(Mg+Fe^{2+})$  vs.  $Cr/(Cr+Al)$  diagrams for ophiolites.

From our own material we can compare the results from Mount Dietrichshorn with more than 500 analyses from Cretaceous clastics of the Western Carpathians (see Jablonský et al. 2001) and they show a perfect match (Fig. 11). Another

perfect match is found in the heavy mineral spectra from Urgonian pebbles (Wagreich et al. 1995), which display strong predominance of Cr-spinels (over 90 %) and they all came exclusively from harzburgitic sources.

1. It indicates that Cretaceous chrome spinels and our analysed samples have the same geochemistry and thus indicate erosion of the same ophiolite nappe stack;

2. Our age data of the sedimentary rock succession thus point to the fact that erosion of the same obducted ophiolite nappe stack started already in the Kimmeridgian and lasted in the study area until the Lower Cretaceous (~Lower Aptian; Rossfeld Fm), in other areas until the Paleogene.

Erosion of the ophiolite nappe stack was interrupted in the time span Late Kimmeridgian to Tithonian by the evolution of a shallow-water carbonate platform, as known, for example, in Albania on top of the Mirdita ophiolites (Schlagintweit et al. 2008) or Greece on top of the Vourinos ophiolite (Carras et al. 2004). Erosion of this platform started around the Jurassic/Cretaceous-boundary as is proven by the occurrence of Late Jurassic shallow-water pebbles in the Early Cretaceous Firza Flysch (Gawlick et al. 2008; Schlagintweit et al. 2008) in Albania, or the Early Cretaceous Bosnian Flysch (Mikes et al. 2008). Reworked pebbles from the different facies belts of this shallow-water platform (similar to the Kurbnesh carbonate platform — Schlagintweit et al. 2008) were recently also described from the Berriasian-Valanginian of the Vardar zone by Kostaki et al. (2013).

The younger, Gosau Group spinels show already a mixed, harzburgitic-Iherzolitic source, but only in the Coniacian to

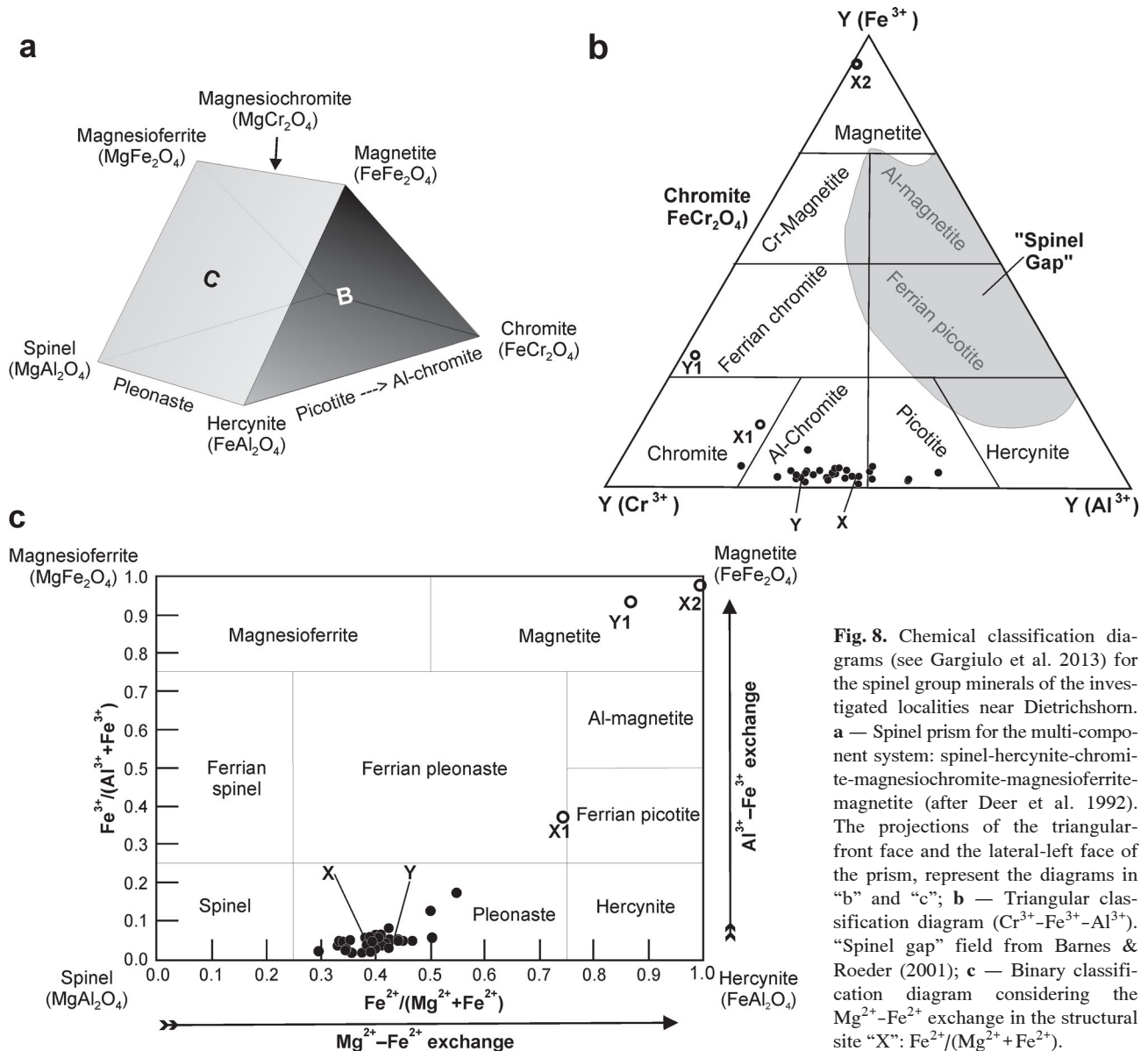


**Fig. 8.** Chemical classification diagrams (see Gargiulo et al. 2013) for the spinel group minerals of the investigated localities near Dietrichshorn. **a** — Spinel prism for the multi-component system: spinel-hercynite-chromite-magnesiochromite-magnesioferrite-magnetite (after Deer et al. 1992). The projections of the triangular-front face and the lateral-left face of the prism, represent the diagrams in "b" and "c"; **b** — Triangular classification diagram ( $\text{Cr}^{3+}$ - $\text{Fe}^{3+}$ - $\text{Al}^{3+}$ ). "Spinel gap" field from Barnes & Roeder (2001); **c** — Binary classification diagram considering the  $\text{Mg}^{2+}$ - $\text{Fe}^{2+}$  exchange in the structural site "X":  $\text{Fe}^{2+}/(\text{Mg}^{2+} + \text{Fe}^{2+})$ .

Campanian samples. In the Maastrichtian it is again exclusively harzburgitic (Stern & Wagerich 2013). Later appearance of lherzolitic material in sediments may indicate progressive erosion, reaching a lower ophiolitic unit that was long-time buried below the upper, harzburgitic nappe.

On the other hand, the present outcrops of primary ophiolitic rocks of the Meliatic and Penninic provenance show mostly lherzolitic origin (Mikuš & Spišiak 2007) and their spinel chemistry is mostly off the range of the samples from Mount Dietrichshorn (Fig. 11). In the present-day position, harzburgitic ophiolites are more common in the Dinaridic and Hellenidic obducted ophiolites, such as the Vourinos harzburgite (Rassios 2008; Rassios et al. 2010). The best example may be the Mirdita ophiolites in Albania, which represent remnants of Mesozoic oceanic lithosphere within the Dinaride-Hellenide segment of the Alpine orogenic system. In the Mirdita ophiolites two different rock associations are distinguished: The Western Ophiolite Belt (WOB) and

the Eastern Ophiolite Belt (EOB) (Beccalova et al. 1994; Bortolotti et al. 2002, 2005; Shallo & Dilek 2003).

The WOB with mainly lherzolitic basement is interpreted as normal oceanic lithosphere whereas the EOB shows harzburgitic basement and is interpreted as (Jurassic) supra-subduction lithosphere formed above an intra-oceanic subduction zone (Shallo & Dilek 2003). The WOB represents Middle Triassic to Early Jurassic Neotethys oceanic crust and occurs in a lower nappe position. The EOB represents late Early to Middle Jurassic SSZ oceanic crust including boninites (Höck et al. 2002; Koller et al. 2006). Due to intra-oceanic stacking and Middle to Late Jurassic obduction the EOB occurs in a higher nappe position than the WOB (Gawlick et al. 2008). Therefore erosion of the EOB ophiolites and equivalents started much earlier than the older Neotethys oceanic crust with the overlying oceanic sediments. Therefore we interpret that in the Kimmeridgian resediments only chrome spinels from this harzburgitic source are found. Resediments from the

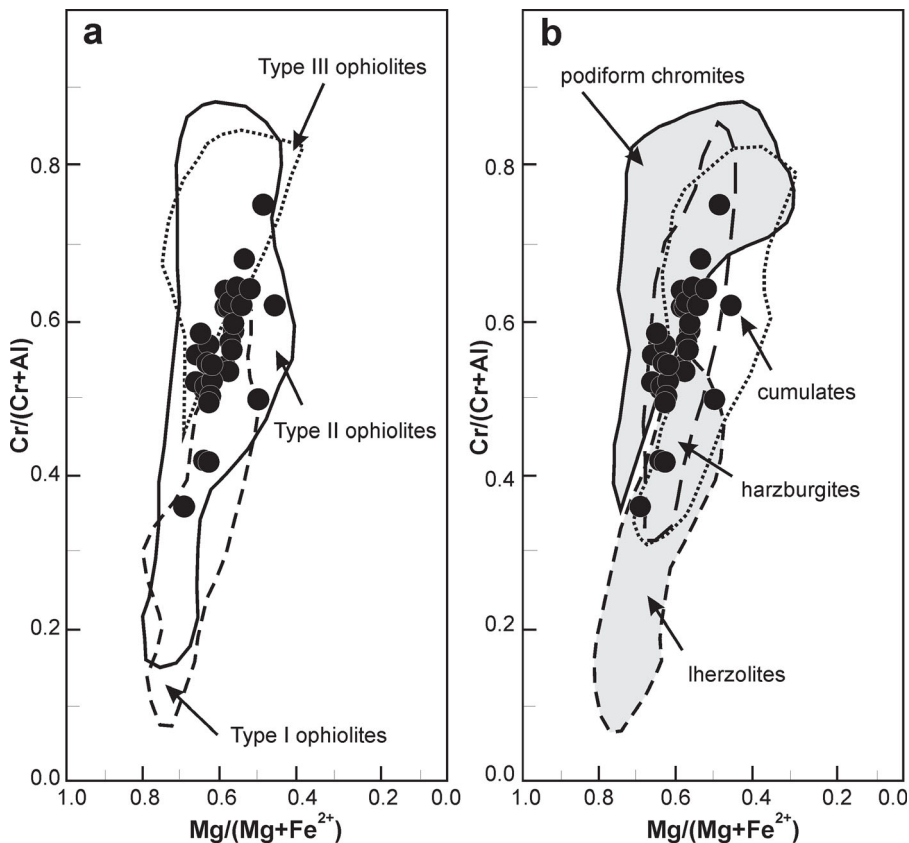


**Fig. 9.** a — Dietrichshorn spinels plotted in the Cr/(Cr+Al) vs. Mg/(Mg+Fe<sup>2+</sup>) diagram with fields distinguished by Dick & Bullen (1984). The vertical distribution of the points best matches to the type II ophiolites; b — the same measurements plotted in the diagram with the fields distinguished by Pober & Faupl (1988). In this diagram, the vertical distribution best matches the field of harzburgites.

Triassic Neotethys oceanic crust are also missing in these Late Jurassic resediments. They become more common in the Lower Cretaceous Rossfeld Formation (Krische et al. 2014) when the erosion cuts deeper into the obducted ophiolitic nappe stack including the subophiolitic mélangé.

Therefore we can use a revised model of the Jurassic geodynamic evolution of the Albanides (Fig. 12), presented by Gawlick et al. (2008), also for the Late Jurassic geodynamic scenario of the Northern Calcareous Alps. However, the provenance area, the ophiolitic nappe stack, originally south of the Northern Calcareous Alps is today completely eroded.

Our finding of ophiolite-derived material already in the Upper Jurassic strata poses the question about relationships of the Late Jurassic and mid-Cretaceous (Eoalpine) orogenic processes, the two events being clearly separated by a comparatively calm phase with development of the Kimmeridgian to earliest Cretaceous carbonate platforms sealing the Jurassic thrust structures and a prolonged period of ophiolite erosion until com-

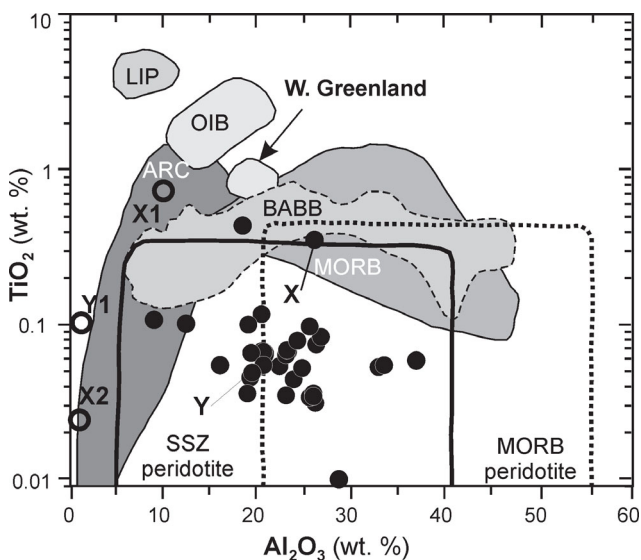


**Fig. 10.** Dietrichshorn spinels plotted in the TiO<sub>2</sub> vs. Al<sub>2</sub>O<sub>3</sub> diagram of Lenaz et al. (2000) and Kamenetsky et al. (2001). **Explanations:** LIP — large igneous provinces, OIB — ocean island basalts, ARC — island-arc magmas, BABB — back-arc basin basalts, MORB — middle ocean ridge Basalts, SSZ — supra-subduction zone peridotites, full circles — fresh spinels, empty circles — altered spinel rims.

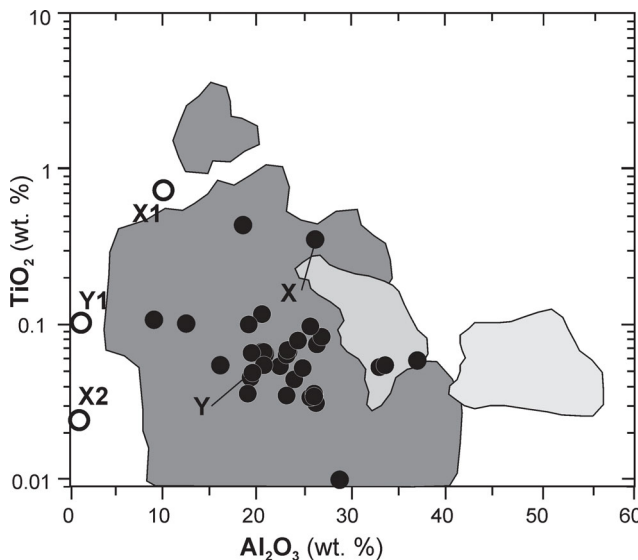


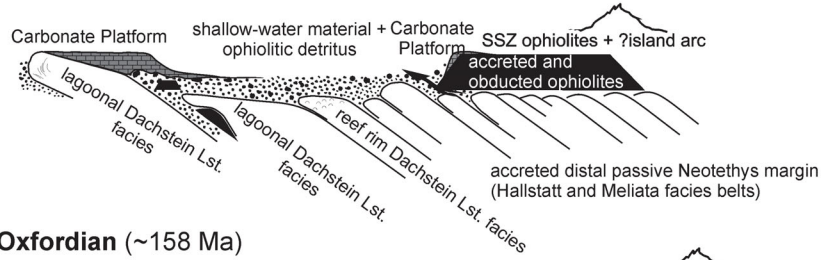
**Fig. 11.** Dietrichshorn spinels plotted in the TiO<sub>2</sub> vs. Al<sub>2</sub>O<sub>3</sub> diagram and compared with spinel chemistry from the West-Carpathian Cretaceous synorogenic sediments (dark grey field, diagram from unpublished data of Jablonský et al. 2001) and Meliatic and Penninic primary ophiolitic outcrops (light-grey fields, data from Mikuš & Spišiák 2007).

NW

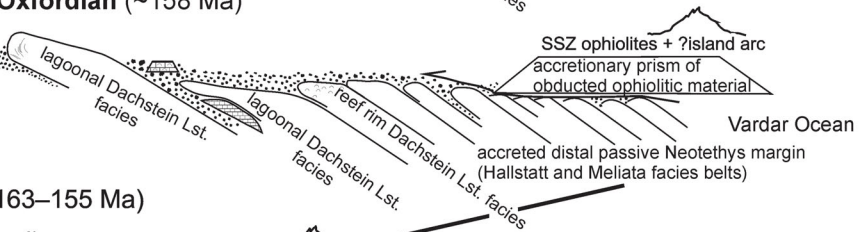
SE

**f**

**Early Kimmeridgian**  
(~154–153 Ma)

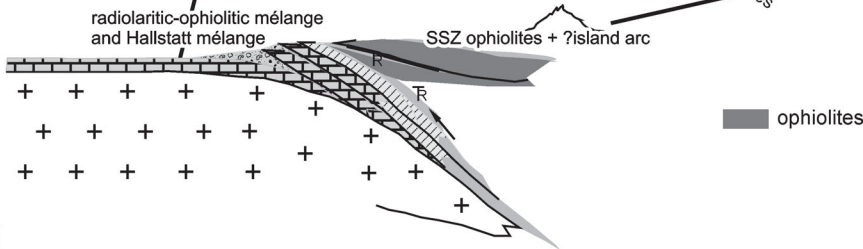


**e1 Middle Oxfordian** (~158 Ma)



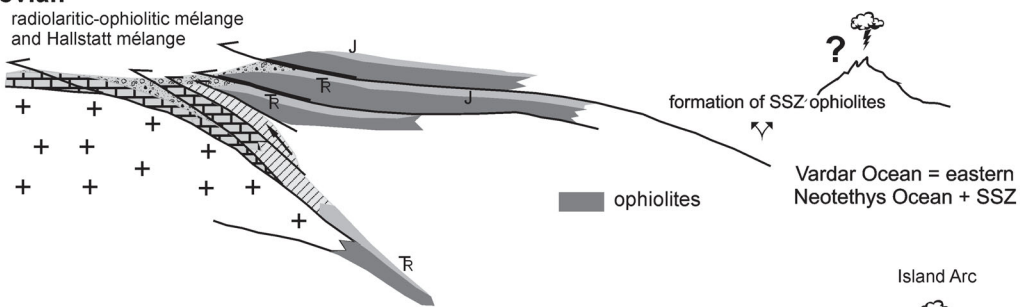
**e**

**Callovian/Oxfordian** (163–155 Ma)



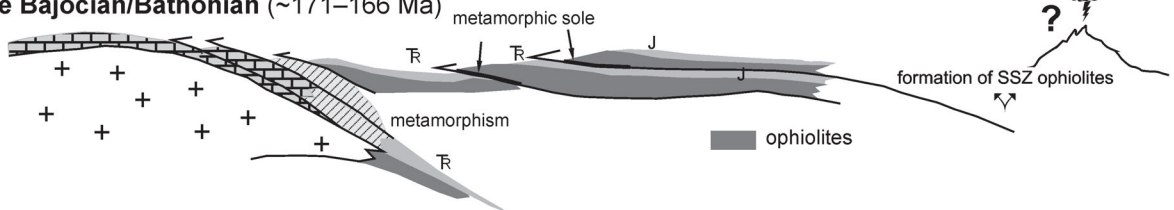
**d**

**Bathonian/Callovian**  
(166–163 Ma)



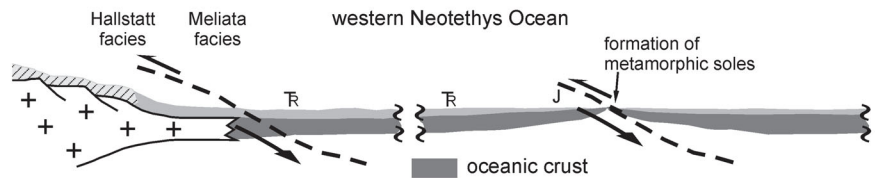
**c**

**late Bajocian/Bathonian** (~171–166 Ma)



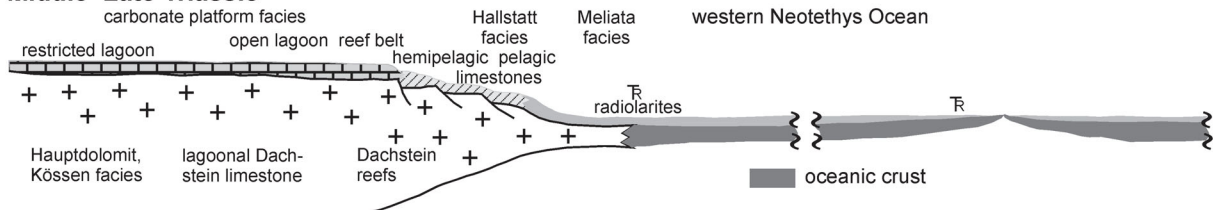
**b**

**late Early Jurassic**  
(~180–175 Ma)



**a**

**Middle–Late Triassic**



mencement of the renewed, Eoalpine shortening at ca. 120 Ma (Early–Middle Aptian). According to the current views (e.g. Janák et al. 2004), the Eoalpine orogeny was initiated by an intracontinental subduction of a belt of dense lower Central Austroalpine crust attenuated by Permian rifting and magmatic underplating. Ensuing convergence and shortening triggered renewed Upper Austroalpine thrust stacking and further erosion of ophiolite-bearing units until their complete elimination from the present surface structure. Consequently, evidence for the existence of this ophiolitic nappe stack in Late Jurassic to Paleogene times south of today's Northern Calcareous Alps comes only from pebble analysis in the Late Jurassic, Early Cretaceous (e.g. van Eynatten & Gaupp 1999; Krische et al. 2014) and Late Cretaceous to Paleogene sedimentary rocks (e.g. Wagreich et al. 1995; Stern et al. 2013). In the Lower Gosau sedimentary rocks of the southeastern Northern Calcareous Alps a complete suite of ophiolite rocks including the Middle Jurassic metamorphic sole (Schuster et al. 2007), together with the whole Middle to Late Triassic oceanic ribbon radiolarite sequence, and of the subophiolitic mélange are proven (Suzuki et al. 2007).

### Conclusions

The new data from detrital chrome spinel grains in the western central Northern Calcareous Alps result in the following conclusions:

1. Erosion of the obducted ophiolite stack started in the Kimmeridgian and not in the Early Cretaceous as previously assumed. This clearly indicates that the first thrusting event related to ophiolite obduction (upper plate) in the Northern Calcareous Alps is of Jurassic age. In a Jurassic strike-slip tectonic environment redeposition of eroded oceanic crust cannot be expected;



**Fig. 12.** Geodynamic reconstruction for the southern Northern Calcareous Alps for Triassic–Jurassic times. Reconstruction of the Triassic shelf configuration after Gawlick et al. (1999). Reconstruction of the Jurassic evolution after Gawlick et al. (1999, 2009), Missoni & Gawlick (2011a,b) for the Northern Calcareous Alps and Gawlick et al. (2008, 2014) for the Dinarides/Albanides on the basis of Kober (1914) concerning the genesis and emplacement of the Mirdita ophiolites and related radiolaritic-ophiolitic trench fills (see also Bortolotti et al. 2005; Schmid et al. 2008; Kiliás et al. 2010). Ages after Gradstein et al. (2004). Middle to Late Triassic Neotethys passive margin configuration (valuable for the Eastern Alps (Austroalpine), Western Carpathians, Southern Alps (Southalpine) and the Dinarides/Albanides) with generation of oceanic crust, and formation of the Toarcian to Oxfordian metamorphic soles due to intra-oceanic subduction, Bajocian to Oxfordian ophiolite obduction and initiation of radiolaritic-ophiolitic trench fills (ophiolitic mélange) deposition and synsedimentary thrusting. Formation of carbonate platforms on top of topographic highs of the nappe stack and the obducted ophiolites started in the latest Oxfordian. During Kimmeridgian–Tithonian times the platform prograded towards the basinal areas and also overlaid the mélanges (compare Fig. 12f and Fig. 3). For discussion, see Robertson & Shallo (2000), Robertson (2006, 2012). **a–e** modified after Gawlick et al. (2008, 2014), **e1–f** modified and simplified after Missoni & Gawlick (2011a,b).

2. The geochemical composition of the detrital chrome spinels points to a harzburgite provenance. The (Jurassic SSZ) ophiolites occur in a higher nappe position than the (mainly) lherzolitic (Triassic) ophiolites, as proven in the ophiolite nappe stack, for example, in Albania (Mirdita ophiolites);

3. The southern Northern Calcareous Alps underwent the same Jurassic to Early Cretaceous geodynamic history as the Western Carpathians, the Dinarides, and the Albanides/Hellenides with Middle to early Late Jurassic ophiolite obduction and the onset of erosion of the ophiolitic nappe pile in the Kimmeridgian. A Kimmeridgian to earliest Cretaceous carbonate platform evolved on top of the nappe stack including the obducted ophiolites. Erosion of the obducted ophiolite nappe stack started in the Kimmeridgian and lasted until the late Early Cretaceous (Aptian), but was interrupted by the (Late) Kimmeridgian to earliest Cretaceous platform evolution, which protected the ophiolite nappe stack against erosion during that time span. In the Early Cretaceous much of this platform was also eroded and can only be reconstructed by pebble analysis from mass flows in the Lower–Upper Cretaceous sedimentary successions.

**Acknowledgments:** Supported by the OeAD WTZ Projects SK 04/2011, SK 08/213 (HJG, SM, RA, DP) and the Projects: APVV SK-AT-0002-12, APVV 0212-12 and VEGA 2/0195/12 (RA, DP). Reviews of Michael Wagreich and anonymous to a previous version of the manuscript and Pavel Uher and 2 additional anonymous reviewers are gratefully acknowledged.

### References

- Árgyelán B.G. 1996: Geochemical investigations of detrital chrome spinels as a tool to detect an ophiolitic source area (Gerecse Mts. Hungary). *Acta Geol. Hung.* 39, 4, 341–368.
- Barnes S.J. & Roedes P.L. 2001: The range of spinel composition in terrestrial mafic and ultramafic rocks. *J. Petrology* 42, 2279–2302.
- Beccaluva V., Coltorti M., Premti I., Saccani E., Sienna F. & Zeda O. 1994: Mid-ocean ridge and supra-subduction affinities in ophiolite belts from Albania. *Ophioliti* 19, 77–96.
- Bortolotti V., Marroni M., Pandolfi L. & Principi G. 2005: Mesozoic and Tertiary tectonic history of the Mirdita ophiolites, northern Albania. *The Island Arc* 14, 471–493.
- Bortolotti V., Marroni M., Pandolfi L., Principi G. & Saccani E. 2002: Alternation of MOR and SSZ basalts in Albanian ophiolites: Evidences of interactions between mid-ocean ridge and subduction-related processes in an infant arc setting. *J. Geol.* 110, 561–576.
- Carras N., Fazzuoli M. & Photiades A. 2004: Transition from carbonate platform to pelagic deposition (Mid Jurassic–Late Cretaceous), Vourinos Massif, northern Greece. *Riv. Ital. Paleont. Stratigr.* 110, 345–355.
- Channell J.E.T., Brandner R., Spieler A. & Smathers N.P. 1990: Mesozoic paleogeography of the Northern Calcareous Alps — Evidence from paleomagnetism and facies analysis. *Geology* 18, 828–831.
- Channell J.E.T., Brandner R., Spieler A. & Stoner J.S. 1992: Paleomagnetism and paleogeography of the Northern Calcareous Alps (Austria). *Tectonics* 11, 792–810.
- Darga R. & Schlagintweit F. 1991: Mikrofazies, Paläontologie und Stratigraphie der Lerchkogelkalke (Tithon–Berrias) des Dietrich-

- horns (Salzburger Land, Nördliche Kalkalpen). *Jb. Geol. Bundesanst.* 134, 205–226.
- Darga R. & Weidich K.F. 1986: Die Lackbach-Schichten, eine klassische Unterkreide-Serie in der Unkenner Mulde (Nördliche Kalkalpen). *Mitt. Bayer. St.-Samml. Paläont. Hist. Geol.* 26, 93–112.
- Deer W.A., Howie R.A. & Zussman J. 1992: An introduction to the rock-forming minerals. *Longman Scientific & Technical*, London, 1–695.
- Dick H.J.B. & Bullen T. 1984: Chromian spinel as a petrogenetic indicator in abyssal and alpine-type peridotites and spatially associated lavas. *Contr. Mineral. Petrology* 86, 54–76.
- Faupl P. & Pober E. 1991: Zur Bedeutung detritischer Chromspinelle in den Ostalpen: Ophiolithischer Detritus aus der Vardarsutur. In: Lobitzer H. & Császár G. (Eds.): *Jubiläumsschrift 20 Jahre Geologische Zusammenarbeit Österreich-Ungarn. Teil 1, Guidebook*. Wien, 133–143.
- Faupl P. & Wagreich M. 2000: Late Jurassic to Eocene Palaeogeography and geodynamic evolution of the eastern Alps. *Mitt. Österr. Geol. Gesell.* 92, 79–94.
- Frank W. 1987: Evolution of the Austroalpine elements in the Cretaceous. In: Flügel H.W. & Faupl P. (Eds.): *Geodynamics of the Eastern Alps. Deuticke*, Wien, 379–406.
- Frank W. & Schlager W. 2006: Jurassic strike slip versus subduction in the Eastern Alps. *Int. J. Earth Sci.* 95, 431–450.
- Frisch W. & Gawlick H.-J. 2003: The nappe structure of the central Northern Calcareous Alps and its disintegration during Miocene tectonic extrusion — a contribution to understanding the orogenic evolution of the Eastern Alps. *Int. J. Earth Sci.* 92, 712–727.
- Fuchs W. 1968: Eine bemerkenswerte, tieferes Apt belegende Foraminiferenfauna aus den konglomeratreichen Oberen Roffeldschichten von Grabenwald (Salzburg). *Verh. Geol. Bundesanst.* 1–2, 87–89.
- Gargiulo M.F., Bjerg E.A. & Mogessie A. 2013: Spinel group minerals in metamorphosed ultramafic rocks from Río de Las Tunas belt, Central Andes, Argentina. *Geol. Acta* 11, 2, 133–148.
- Gawlick H.-J. & Frisch W. 2003: The Middle to Late Jurassic carbonate clastic radiolaritic flysch sediments in the Northern Calcareous Alps: sedimentology, basin evolution and tectonics — an overview. *Neu. Jb. Geol. Paläont., Abh.* 230, 163–213.
- Gawlick H.-J., Missoni S., Schlagintweit F. & Suzuki H. 2012: Jurassic active continental margin deep-water basin and carbonate platform formation in the north-western Tethyan realm (Austria, Germany). *J. Alp. Geol.* 54, 89–292.
- Gawlick H.-J., Frisch W., Vecsei A., Steiger T. & Böhm F. 1999: The change from rifting to thrusting in the Northern Calcareous Alps as recorded in Jurassic sediments. *Geol. Rundsch.* 87, 644–657.
- Gawlick H.-J., Lein R., Missoni S., Krystyn L., Frisch W. & Hoxha L. 2014: The radiolaritic-argillaceous Kcira-Dushi-Komani sub-ophiolitic Hallstatt Mélange in the Mirdita Zone of Northern Albania. *Bul. Shkenc. Gjeol., Spec. Issue* 4, 1–32.
- Gawlick H.-J., Frisch W., Hoxha L., Dumitrică P., Krystyn L., Lein R., Missoni S. & Schlagintweit F. 2008: Mirdita Zone ophiolites and associated sediments in Albania reveal Neotethys Ocean origin. *Int. J. Earth Sci.* 97, 865–881.
- Gawlick H.-J., Missoni S., Schlagintweit F., Suzuki H., Frisch W., Krystyn L., Blau J. & Lein R. 2009: Jurassic tectonostratigraphy of the Austroalpine domain. *J. Alp. Geol.* 50, 1–152.
- Gradstein F., Ogg J. & Smith A. 2004: A Geological Time Scale. *Cambridge University Press*, Cambridge, 1–610.
- Haas J., Kovács S., Gawlick H.-J., Grădinaru E., Karamata S., Sudar M., Péró C., Mello J., Polák M., Ogorelec B. & Buser S. 2011: Jurassic evolution of the tectonostratigraphic units of the Circum-Pannonian Region. *Jb. Geol. Bundesanst.* 151, 281–354.
- Haggerty S.E. 1991: Oxide mineralogy of the upper mantle. Spinel mineral group. In: Lindsley D.H. (Ed.): *Oxide minerals: Petrologic and magnetic significance. Rev. in Mineralogy* 25, *Mineral. Soc. Amer.*, 355–416.
- Höck V., Koller F., Meisel T., Onuzi K., Gjata K. & Kneringer E. 2002: The South Albanian ophiolites: MOR versus SSZ ophiolites. *Lithos* 65, 143–165.
- Jablonský J., Sýkora M. & Aubrecht R. 2001: Detritic Cr-spinels in Mesozoic sedimentary rocks of the Western Carpathians (overview of the latest knowledge). *Miner. Slovaca* 33, 5, 487–498 (in Slovak with English summary).
- Janák M., Froitzheim N., Lupták B., Vrabec M. & Krogh Ravna E.J. 2004: First evidence for ultrahigh-pressure metamorphism of eclogites in Pohorje, Slovenia: Tracing deep continental subduction in the Eastern Alps. *Tectonics* 23, TC514.
- Kamenetsky V.S., Crawford A.J. & Meffre S. 2001: Factors controlling chemistry of magmatic spinel: an empirical study of associated olivine, Cr-spinel and melt inclusion from primitive rocks. *J. Petrology* 42, 655–671.
- Kilias A., Frisch W., Avgerinas A., Dunkl I., Falalakis G. & Gawlick H.-J. 2010: Alpine architecture and kinematics of deformation of the Northern Pelagonian nappe pile in Hellenides. *Aust. J. Earth Sci.* 103, 4–28.
- Kober L. 1914: Die Bewegungsrichtung der alpinen Deckengebirge des Mittelmeeres. *Petermann's Geograph. Mitt.* 60, 250–256.
- Koller F., Höck V., Meisel T., Ionescu C., Onuzi K. & Ghega D. 2006: Cumulates and gabbros in southern Albanian ophiolites: their bearing on regional tectonic setting. In: Robertson A.H.F. & Mountrakis D. (Eds.): *Tectonic development of the Eastern Mediterranean Region. Geol. Soc. London, Spec. Publ.* 260, 267–299.
- Kostaki G., Kilias A., Gawlick H.-J. & Schlagintweit F. 2013: ?Kimmeridgian–Tithonian shallow-water platform clasts from mass flows on top of the Vardar/Axios ophiolites. *Bull. Geol. Soc. Greece* XLVII, 184–193.
- Kralik M., Krumm H. & Schramm J.M. 1987: Low grade and very low grade metamorphism in the Northern Calcareous Alps and in the greywacke zone: Illite-crystallinity data and isotopic ages. In: Flügel H.W. & Faupl P. (Eds.): *Geodynamics of the Eastern Alps. Deuticke*, Wien, 165–178.
- Krische O., Goričan Š. & Gawlick H.-J. 2014: Erosion of a Jurassic ophiolitic nappe-stack as indicated by exotic components in the Lower Cretaceous Rossfeld Formation of the central Northern Calcareous Alps (Austria). *Geol. Carpathica* 65, 3–24.
- Lenaz D., Kamenetsky V.S., Crawford A.J. & Princivalle F. 2000: Melt inclusion in detrital spinel from the SE Alps (Italy–Slovenia): a new approach to provenance studies of sedimentary basins. *Contr. Mineral. Petrology* 139, 748–758.
- Lenaz D., Mazzoli C., Spišiak J., Princivalle F. & Maritan L. 2009: Detrital Cr-spinel in the Šambron-Kamenica Zone (Slovakia): evidence for an ocean-spreading zone in the Northern Vardar suture? *Int. J. Earth Sci.* 98, 345–355.
- Lužar-Oberiter B., Mikes T., von Eynatten H. & Babić L. 2009: Ophiolitic detritus in Cretaceous clastic formations of the Dinarides: Ophiolitic detritus in Cretaceous clastic formations of the Dinarides (NW Croatia): evidence from Cr-spinel chemistry. *Int. J. Earth Sci.* 98, 1097–1108.
- Mandl G.W. 2000: The Alpine sector of the Tethyan shelf — examples of Triassic to Jurassic sedimentation and deformation from the Northern Calcareous Alps. *Mitt. Österr. Geol. Gesell.* 92, 61–77.
- Mandl G.W. 2013: Zur Geologie des Raumes Hütteneckalm-Sandlingalm-Blaa-Alm (Salzkammergut, Österreich) mit kritischen Anmerkungen zur Sandlingalm-Formation. *Jb. Geol. Bundesanst.* 153, 33–74.
- Mikes T., Christ D., Petri R., Dunkl I., Frei D., Báldi-Béke M.,

- Reitner J., Wemmer K., Hrvatović H. & von Eynatten H. 2008: Provenance of the Bosnian Flysch. *Swiss J. Geosci.* 101, 1, 31–54.
- Mikuš T. & Spišiak J. 2007: Chemical composition and alteration of Cr-spinels from Meliata and Penninic serpentized peridotites (Western Carpathians and Eastern Alps). *Geol. Quart.* 51, 257–270.
- Missoni S. & Gawlick H.-J. 2010: Neudefinition der Saalachzone in den Nördlichen Kalkalpen (Österreich, Deutschland): was ist sie, woher kommt sie und woraus besteht sie? *J. Alp. Geol.* 52, 182–184.
- Missoni S. & Gawlick H.-J. 2011a: Evidence for Jurassic subduction from the Northern Calcareous Alps (Berchtesgaden; Austroalpine, Germany). *Int. J. Earth Sci.* 100, 1605–1631.
- Missoni S. & Gawlick H.-J. 2011b: Jurassic mountain building and Mesozoic–Cenozoic geodynamic evolution of the Northern Calcareous Alps as proven in the Berchtesgaden Alps (Germany). *Facies* 57, 137–186.
- Missoni S., Schlagintweit F., Suzuki H. & Gawlick H.-J. 2001: Die oberjurassische Karbonatplattformentwicklung im Bereich der Berchtesgadener Kalkalpen (Deutschland) — eine Rekonstruktion auf der Basis von Untersuchungen polymikter Brekzienkörper in pelagischen Kieselsteinen (Sillenkopf-Formation). *Zbl. Geol. Paläont., Teil I* 1, 2, 117–143.
- Ortner H., Ustaszewski M. & Rittner M. 2008: Late Jurassic tectonics and sedimentation: breccias in the Unken syncline, central Northern Calcareous Alps. *Swiss J. Geosci.* 101, Suppl. 1, S55–S71.
- Pestal G., Hejl E., Braunstingl R. & Schuster R. (Eds.) 2009: Erläuterungen Geologische Karte von Salzburg 1:200,000. *Geol. Bundesanst.*, Wien, 1–162.
- Pober E. & Faupl P. 1988: The chemistry of detrital chromian spinels and its implications for the geodynamic evolution of the Eastern Alps. *Geol. Rdsch.* 77, 671–670.
- Power M.R., Pirrie D., Andersen J.C. & Wheeler P.D. 2000: Testing the validity of chrome spinel chemistry as a provenance and petrogenetic indicator. *Geology* 28, 1027–1030.
- Quast P., Maxl M., Suzuki H., Missoni S. & Gawlick H.-J. 2010: Matrixalter der Hallstatt Mélange der Saalachzone (Nördliche Kalkalpen, Österreich). *J. Alp. Geol.* 52, 206–207.
- Rassios A.E. 2008: A geologist's guide to West Macedonia, Greece. *The Grevena Development Agency, Inst. Geol. Miner. Deposits*, Kozani, Greece, 1–119.
- Rassios A.E., Kostopoulos D. & Dilek Y. 2010: Exhumation of the West Pelagonian margin and Pindos basin emplacement. *XIX Congress CBGA, Thessaloniki, Greece, 23–26 September, 2010, Field-trip guide*, 1–62.
- Robertson A.H.F. 2006: Contrasting modes of ophiolite emplacement in the Eastern Mediterranean region. In: Gee D.G. & Stephenson R.A. (Eds.): European lithosphere dynamics. *Geol. Soc. Mem.* 32, 235–262.
- Robertson A.H.F. 2012: Late Palaeozoic–Cenozoic tectonic development of Greece and Albania in the context of alternative reconstructions of Tethys in the Eastern Mediterranean region. *Int. Geol. Rev.* 54, 373–454.
- Robertson A.H.F. & Shallo M. 2000: Mesozoic–Tertiary tectonic evolution of Albania in its regional Eastern Mediterranean context. *Tectonophysics* 316, 197–254.
- Schlagintweit F., Gawlick H.-J. & Lein R. 2005: Mikropaläontologie und Biostratigraphie der Plassen-Karbonatplattform der Typokalitaet (Ober-Jura bis Unter-Kreide, Salzkammergut, Österreich). *J. Alp. Geol., Mitt. Gesell. Geol. Bergbaustud. Österr.* 47, 11–102.
- Schlagintweit F., Krische O. & Gawlick H.-J. 2012: First findings of Orbitolinids (Larger Benthic Foraminifera) from the Early Cretaceous Rossfeld Formation (Northern Calcareous Alps, Austria). *Jb. Geol. Bundesanst.* 152, 145–158.
- Schlagintweit F., Gawlick H.-J., Missoni S., Hoxha L., Lein R. & Frisch W. 2008: The eroded Late Jurassic Kurbnesh carbonate platform in the Mirdita Ophiolite Zone of Albania and its bearing on the Jurassic orogeny of the Neotethys realm. *Swiss J. Geosci.* 101, 125–138.
- Schmid S.M., Bernoulli D., Fügenschuh B., Matenco L., Schefer S., Schuster R., Tischler M. & Ustaszewski K. 2008: The Alpine-Carpathian-Dinaridic orogenic system: correlation and evolution of tectonic units. *Swiss J. Geosci.* 101, 139–184.
- Schorn A., Neubauer F. & Bernroider M. 2013: Polyhalite microfabrics in an Alpine evaporite Mélange: Hallstatt, Eastern Alps. *J. Struct. Geol.* 46, 57–75.
- Schuster R., Koller F. & Frank W. 2007: Pebbles of upper-amphibolite facies amphibolites of the Gosau Group from the Eastern Alps: relics of a metamorphic sole? *8<sup>th</sup> Workshop on Alpine Geological Studies, Abstract volume*, Davos, 1–74.
- Shallo M. & Dilek Y. 2003: Development of the ideas on the origin of Albanian ophiolites. *Geol. Soc. Amer., Spec. Pap.* 373, 351–363.
- Stern G. & Wagneich M. 2013: Provenance of the Upper Cretaceous to Eocene Gosau Group around and beneath the Vienna Basin (Austria and Slovakia). *Swiss J. Geosci.* 106, 3, 505–527.
- Stevens R.E. 1944: Composition of some chromites of the Western Hemisphere. *Amer. Mineralogist* 29, 1–34.
- Suzuki H., Schuster R., Gawlick H.-J., Lein R. & Faupl P. 2007: Neotethys derived obducted ophiolite nappes in the Eastern Alps: informations from radiolarite pebbles in the Gosau Group. *8<sup>th</sup> Workshop on Alpine Geological Studies, Abstract Volume*, Davos, 79–80.
- Thöni M. 2006: Dating eclogite-facies metamorphism in the Eastern Alps — approaches, results, interpretations: a review. *Miner. Petrology* 88, 123–148.
- Tollmann A. 1977: Geologie von Österreich. Band 1. *Deuticke*, Wien, 1–766.
- Tollmann A. 1985: Geologie von Österreich. Band 2. *Deuticke*, Wien, 1–710.
- von Eynatten H. & Gaupp R. 1999: Provenance of Cretaceous synorogenic sandstones in the Eastern Alps: constraints from framework petrography, heavy mineral analysis and mineral chemistry. *Sed. Geol.* 124, 81–111.
- Wagneich M., Faupl P. & Schlagintweit F. 1995: Heavy minerals from Urgonian Limestone pebbles of the Northern Calcareous Alps (Austria, Bavaria): further evidence for an intra-Austroalpine suture zone. *Geol. Carpathica* 46, 197–204.
- Weidich K. 1990: Die kalkalpine Unterkreide und ihre Foraminiferfauna. *Zitteliana* 17, 1–312.